Sildenafil Potentiates the Therapeutic Efficacy of Docetaxel in Advanced Prostate Cancer by Stimulating NO-cGMP Signaling

Sakthivel Muniyan[1], Satyanarayana Rachagani[1], Seema Parte[1], Sushanta Halder[1], Parthasarathy Seshacharyulu[1], Prakash Kshirsagar[1], Jawed A. Siddiqui[1], Raghupathy Vengoji[1], Sanchita Rauth[1], Ridwan Islam[1], Kavita Mallya[1], Kaustubh Datta[1,2], Lei Xi[3], Anindita Das[3], Benjamin A. Teply[2,4], Rakesh C. Kukreja[3], and Surinder K. Batra[1,2,5]

ABSTRACT

Purpose: Docetaxel plays an indispensable role in the management of advanced prostate cancer. However, more than half of patients do not respond to docetaxel, and those good responders frequently experience significant cumulative toxicity, which limits its dose duration and intensity. Hence, a second agent that could increase the initial efficacy of docetaxel and maintain tolerability at biologically effective doses may improve outcomes for patients.

Experimental Design: We determined phosphodiesterase 5 (PDE5) expression levels in human and genetically engineered mouse (GEM) prostate tissues and tumor-derived cell lines. Furthermore, we investigated the therapeutic benefits and underlying mechanism of PDE5 inhibitor sildenafil in combination with docetaxel using *in vitro*, Pten conditional knockout (cKO), derived tumoroid and xenograft prostate cancer models.

Results: PDE5 expression was higher in both human and mouse prostate tumors and cancer cell lines compared with normal tissues/cells. In GEM prostate-derived cell lines, PDE5 expression increased from normal prostate (wild-type) epithelial cells to androgen-dependent and castrated prostate-derived cell lines. The addition of physiologically achievable concentrations of sildenafil enhanced docetaxel-induced prostate cancer cell growth inhibition and apoptosis *in vitro*, reduced murine 3D tumoroid growth, and *in vivo* tumorigenicity as compared with docetaxel alone. Furthermore, sildenafil enhanced docetaxel-induced NO and cGMP levels thereby augmenting antitumor activity.

Conclusions: Our results demonstrate that sildenafil's addition could sensitize docetaxel chemotherapy in prostate cancer cells at much lesser concentration than needed for inducing cell death. Thus, the combinatorial treatment of sildenafil and docetaxel may improve anticancer efficacy and reduce chemotherapy-induced side-effects among patients with advanced prostate cancer.

Introduction

Docetaxel, along with prednisone, has been the standard of care first-line chemotherapy for metastatic castration-resistant prostate cancer (mCRPC) since 2004 (1, 2). The cytotoxic effect of docetaxel is mainly mediated by mitotic catastrophe by inducing G_2–M arrest (3). However, many tumors do not respond, and most patients develop resistance (2). Even among patients who have tumor response, drug-related adverse effects are frequent (4), which eventually leads to limitations in the dose and duration of docetaxel treatment. On the other hand, a recent meta-analysis revealed that prolonged docetaxel treatment (eight or more vs. six cycles) is associated with superior survival among patients with prostate cancer (5). All this evidence suggests that several factors contribute to limited docetaxel efficacy among prostate cancer, and insufficient concentration of intratumoral docetaxel may be one of the reasons for reduced therapeutic outcomes (6).

To augment the efficacy of docetaxel, various combinatorial approaches, including VEGF inhibitors, lenalidomide, dasatinib, endothelin receptor antagonists, and calcitriol, have been employed in clinical trials for advanced prostate cancer (7, 8). However, no randomized study with these combinations showed superiority over docetaxel alone. While there is a growing treatment armamentarium for mCRPC beyond docetaxel, the tumors become progressively more aggressive, and patients ultimately succumb to the disease (9). Hence, we sought to identify a combinational agent that would improve the efficacy of docetaxel by improving dose intensity and duration.

Recently, there has been considerable interest in drug repurposing for disease conditions such as cancer. Sildenafil is a cGMP-specific phosphodiesterase type 5 (PDE5) inhibitor and is clinically approved for the treatment of erectile dysfunction and pulmonary hypertension (PAH). Studies have shown that PDE5 expression is increased in human breast carcinomas (10), bladder squamous carcinoma (11), and multiple cancer cell lines (10–13), suggesting its potential role in controlling tumor cell growth and apoptosis. Recent exploratory and preclinical studies have demonstrated the antitumorigenic potential of sildenafil either by itself or through enhancing the efficacy of other chemotherapeutic drugs in various cancers (14–17). Studies also have shown that sildenafil enhances the delivery of chemotherapeutics in the tumor (18). Furthermore, sildenafil prevented

[1]Department of Biochemistry and Molecular Biology, University of Nebraska Medical Center, Omaha, Nebraska. [2]Fred and Pamela Buffett Cancer Center, Eppley Institute for Research in Cancer and Allied Diseases, University of Nebraska Medical Center, Omaha, Nebraska. [3]Pauley Heart Center, Department of Internal Medicine, Division of Cardiology, Virginia Commonwealth University, Richmond, Virginia. [4]Department of Internal Medicine, University of Nebraska Medical Center, Omaha, Nebraska. [5]Department of Pathology and Microbiology, University of Nebraska Medical Center, Omaha, Nebraska.

Note: Supplementary data for this article are available at Clinical Cancer Research Online (http://clincancerres.aacrjournals.org/).

Corresponding Authors: Surinder K. Batra, University of Nebraska Medical Center, Omaha, NE 68198-5870. Phone: 402-559-5455; Fax: 402-559-6650; E-mail: sbatra@unmc.edu and Sakthivel Muniyan, University of Nebraska Medical Center, Omaha, NE 68198-5870. E-mail: s.muniyan@unmc.edu.

Clin Cancer Res 2020;26:5720–34

doi: 10.1158/1078-0432.CCR-20-1569

©2020 American Association for Cancer Research.

Downloaded from http://aacrjournals.org/clincancerres/article-pdf/26/21/5720/2064320/5720.pdf by guest on 28 August 2022

Translational Relevance

Docetaxel, as a monotherapy, and in combination with hormonal therapy, plays an indispensable role in the management of prostate cancer. However, more than half of the patients show tumor nonresponsiveness; even those responders are frequently associated with significant cumulative toxicity, which limits dose duration and intensity. Our results show that the addition of sildenafil synergistically enhanced docetaxel efficacy by affecting prostate cancer cell growth, inducing apoptosis. Furthermore, the combination treatment reduced growth of Pten conditional knockout mouse-derived tumoroid growth and *in vivo* tumors. Interestingly, sildenafil alone did not affect tumor growth or prostate cancer cell proliferation. Mechanistically, sildenafil stabilized docetaxel-induced NO/cGMP levels to enhance the antitumorigenic effect through PKG/JNK signaling. Our results suggest that combining the taxanes and sildenafil with known pharmacokinetics would lead to better therapeutic benefit with lesser dose, and eventually lower toxicity than usual. Because both the drugs are FDA approved, these results suggest further clinical evaluation of this combination in patients with advanced prostate cancer.

doxorubicin-induced cardiotoxicity in mice bearing prostate cancer (15). Supportively, an epidemiologic study found that patients who received sildenafil for erectile dysfunction had reduced the incidence of prostate cancer (19).

Encouraged by these observations, we investigated whether sildenafil could increase the therapeutic efficacy of docetaxel in advanced prostate cancer and examined possible mechanisms of synergy. To do this, we evaluated the antitumor activity of sildenafil and docetaxel in combination. The therapeutic potential of sildenafil and docetaxel was assessed in multiple androgen receptor (AR)-positive human and mouse prostate cancer cell lines *in vitro*, Pten cKO–derived tumoroids, and *in vivo* xenograft model. In addition, the synergistic effect and its underlying mechanisms were investigated in an *in vitro* system. Our results show that the addition of sildenafil could sensitize prostate cancer cells to docetaxel chemotherapy at a lower concentration than needed for inducing cell death.

Materials and Methods

Cell culture

Human prostate cancer (LNCaP-FGC, C4-2B, 22Rv1, and VCaP) cell lines were originally obtained from ATCC or our collaborators. Cells were maintained in an incubator with 5% CO_2 at 37°C and routinely tested for short tandem repeat (STR) profiles and *Mycoplasma* contamination as described previously (20–23). All the prostate cancer cell lines were authenticated in October 2018 before the start of experiments and the VCaP cell line was obtained from ATCC in December 2019. LNCaP-C-33, C4-2B, and 22Rv1 prostate cancer cells were cultured in RPMI1640 medium supplemented with 5% or 10% FBS and penicillin/streptomycin. VCaP prostate cancer cells were cultured in DMEM supplemented with 10% FBS, and penicillin–streptomycin. PTEN conditional knockout (cKO) mouse-derived E2, E4, cE1, and cE2 prostate cancer cells were a kind gift from Dr. Burman (24). OCT161 cells were derived from the $Pten^{wt}$ mouse (23). All the mouse prostate-derived cells were maintained in DMEM and validated for functional analyses, as described previously (23, 24).

Nitric oxide determination

The relative nitric oxide (NO) levels were determined using 4-amino-5-methylamino-2′,7′-difluorescein diacetate (DAF-FM diacetate; Invitrogen). In brief, cells were incubated with different concentrations of docetaxel for 1 hour in serum-free, phenol red–free culture conditions. For NO determination, 2 μmol/L of DAF-FM diacetate was added and incubated along with the docetaxel. Controls included no drug and no dye conditions. The docetaxel-induced relative benzotriazole fluorescence intensity was measured using a fluorescence plate reader (BioTek's Synergy Neo2). Alternatively, the NO-derived fluorescence was captured using the EVOS FL Cell Imaging System (Invitrogen).

cGMP determination

Intracellular cGMP levels in prostate cancer cells were measured using an ELISA Kit (Cayman Chemical). For measuring cGMP, approximately 5×10^5 cells were plated and cultured for 72 hours. Cells were then washed and incubated in serum-free RPMI media containing vehicle, docetaxel, and sildenafil alone or in combination for 30 minutes. After lysis with 0.1 mol/L HCl, the nonenzymatic conversion of 5,5′-dithio-bis(2-nitrobenzoic acid) into 5-thio-2-nitrobenzoic acid was determined using a UV visible spectrophotometer (Spectra Max 5). Cells were also incubated with NO donor DEA as a positive control. A standard curve was run along with the samples, and the results were expressed as pmol/μg protein.

Gene expression analyses

For PCR and quantitative real-time PCR (qRT-PCR), total RNA was isolated (Qiagen kit), and cDNA was made with random hexamers. For conventional PCR, 50 ng of cDNA was combined with respective primers, DNA polymerase, dNTPs, and buffer. PCR amplification was performed, and the product was electrophoresed in a 2% agarose gel. The Real-Time PCR System (Bio-Rad) was used for gene expression analysis with approximately 20 ng of cDNA mixed with respective primers (Supplementary Table S1) and SYBR Green (Roche).

Cell growth and clonogenic cell survival analysis

To determine the effective dose of docetaxel, sildenafil, and the combination on prostate cancer cell proliferation, LNCaP, C4-2B, and 22Rv1 PCa cells were seeded on 96-well plates at a density of 5×10^3 cells per well. Then, the cells were treated with varying concentrations of docetaxel and sildenafil alone or in combination for 72 hours, with the replacement of drugs every 24 hours. The effects of dose on growth inhibition and proliferation rate were determined using MTT or the trypan blue dye exclusion assay (20). VCaP cell proliferation rate was determined using calcein-AM (Millipore Sigma) by fluorescent plate reader. In brief, after the desired treatment period, the cells were incubated with 200 nmol/L calcein-AM for 30 minutes and the calcein fluorescence intensity was recorded at Ex_{485}/Em_{525} nm using a fluorescent plate reader (BioTek's Synergy Neo2). The lethal dose, effective inhibitory concentration, and synergistic effect of the drug combination were determined by the Chou-Talalay method (25). A combination index (CI) of <1, equal to 1 and >1 indicate synergistic, additive, or antagonistic effects, respectively (25). Furthermore, to determine the therapeutic efficacy of docetaxel and sildenafil combination, a clonogenic cell survival assay was performed as described previously (22). Relative colony growth were determined by manual counting or by measuring the relative intensity of stained colonies using a plate reader at 570 nm (Spectra Max 5; ref. 26).

Downloaded from http://aacrjournals.org/clincancerres/article-pdf/26/21/5720/2064320/5720.pdf by guest on 28 August 2022

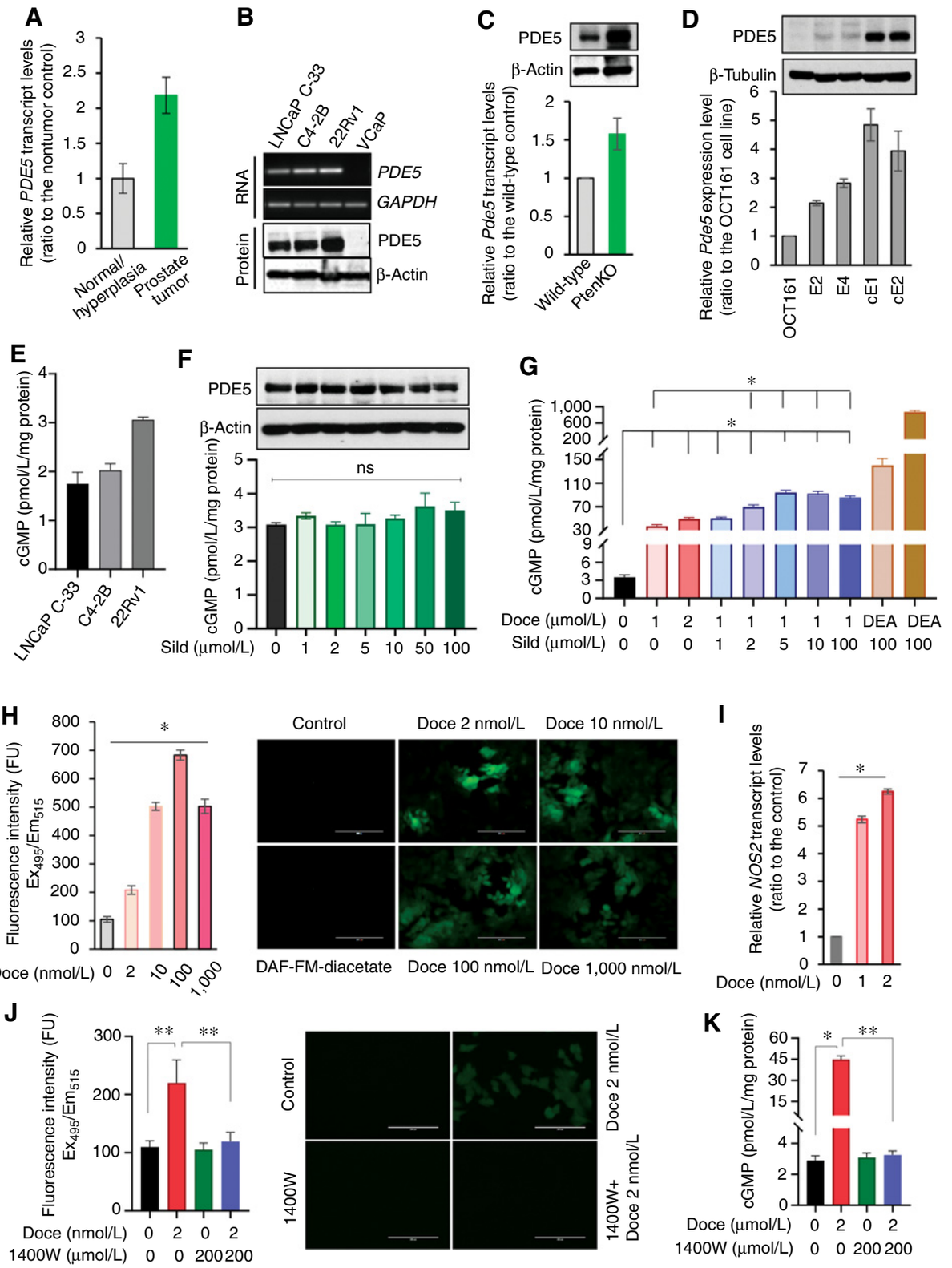

Figure 1.

Docetaxel-induced NO levels were stabilized by sildenafil in prostate cancer. **A,** RT-PCR analyses to determine the relative *PDE5* expression levels in human prostate cancer samples ($n = 41$) compared with nontumor ($n = 9$) samples. The results presented are normalized to *GAPDH* mRNA levels. **B,** PDE5 expression levels were determined in the human prostate cancer cell lines used in this study by qRT-PCR and Western blot analyses. (*Continued on the following page.*)

Downloaded from http://aacrjournals.org/clincancerres/article-pdf/26/21/5720/2064320/5720.pdf by guest on 28 August 2022

FACS analyses

For cell-cycle distribution, prostate cancer cells stained with Telford reagent for 30 minutes at room temperature and moved to ice until analysis by FACS (20). The singlets were analyzed for cells in different cell-cycle phases using ModFit software. The number of apoptotic prostate cancer cells was also determined in the sub-G_0–G_1 population, as described previously (20). The apoptotic population using Annexin-V and 7-AAD staining in prostate cancer cells was performed by FACS. The detailed protocol for cell-cycle and annexin V assays are given in the Supplementary Materials and Methods.

Mitochondrial permeability transition pore assay

Mitochondrial permeability transition pore (MPTP) activity was analyzed using calcein-AM and $CoCl_2$. In brief, 22Rv1 prostate cancer cells were plated in a 96-well plate and treated for 48 hours as described above. After that, the medium was removed, and attached cells were carefully washed with PBS and incubated with 100 nmol/L calcein-AM. In additional wells, 100 μmol/L $CoCl_2$ was added and incubated for 30 minutes at 37°C to quench the cytosolic calcein. Cells were finally washed with PBS, and the intracellular calcein fluorescence intensity was measured using a fluorescence plate reader (BioTek Synergy Neo 2).

Real-time annexin-V apoptosis and necrosis assay

The real-time apoptosis and necrosis assay in VCaP cells were performed as per manufacturer's instructions (No. JA1012, Promega). In brief, VCaP prostate cancer cells were seeded at the density of 5,000 cells in Corning white-walled clear TC-treated 96-well plates and incubated for 24 hours at 37°C in a CO_2 incubator. After 24 hours, the drugs either alone or in the combination were added along with $CaCl_2$ and Annexin V NanoBiT substrate. After 2 hours, other reagent mixtures were added, and the fluorescence or luminescence intensities were monitored continuously for 24 hours. Every 24 hours, along with the treatment compounds, the apoptosis and necrosis reagent mixtures were replaced and monitored for either apoptosis or necrosis. Baseline absorbance, cells alone, and no cell reagents control were maintained and corrected for the baseline fluorescence and luminescence intensity (BioTek Synergy Neo 2).

Transient knockdown of PDE5

PDE5-specific or control siRNA (Santa Cruz Biotechnology) at a concentration of 100 nmol/L was transiently transfected into 22Rv1 cells using Lipofectamine 2000 as per manufacturer's instructions (Invitrogen). After 6 hours, the transfected cells received a complete medium. Twenty-four hours later, the transfection procedure was repeated to achieve maximal knockdown, and the cells were harvested at the end of 72 hours. Transfected cells were maintained in the presence and absence of docetaxel to determine the additive effect of PDE5 inhibition on PARP cleavage.

Immunoblot analyses

Treated cells were washed and lysed with RIPA buffer containing protease and phosphatase inhibitors. Lysates were freeze-thawed, syringe passaged, and centrifuged at 13,000 rpm for 25 minutes at 4°C. To determine protein expression levels, equal amounts of protein (40 μg) were subjected to immunoblot analyses. The immobilized proteins were incubated with respective primary antibodies (Supplementary Table S2). The membranes were probed with respective secondary antibodies for an hour before capturing expression with enhanced chemiluminescence reagent.

Pten cKO–derived tumoroid and scaffold-free 3D culture

Pten cKO–derived tumoroids used in this study were generated, and the treatment strategy is as described in our recent publications (23). The tumoroid were treated with either docetaxel or sildenafil alone or the combination and the therapeutic impact was monitored every 24 hours by measuring the tumoroid size (EVOS Imaging System, Invitrogen). For 3D culture, mouse-derived cE2 cells were plated in Ultra-low Attachment Plate (S-BIO). After 48 hours of the cell forming 3D colony, the cells received either docetaxel or sildenafil alone or the combination for 20 consecutive days. The 3D colonies were monitored every 48 hours for the impact of combination treatment on colony growth. On day 20, the colonies were incubated with calcein-AM and the resulting green fluorescence was recorded (BioTek Synergy Neo2).

In vivo xenograft study

Immunocompromised male athymic nude mice were obtained from our in-house breeding colony. Animal experiments were conducted by guidelines and protocol approved by the Institutional Animal Care and Use Committees (IACUC) of the University of Nebraska Medical Center (Omaha, Nebraska). All mice were housed in a well-ventilated, pathogen-free cages, with access to food and water *ad libitum*. In brief, approximately 2×10^5 luciferase-transfected C4-2B prostate cancer cells were mixed with matrigel (BD Biosciences) and implanted into the dorsolateral lobe of the mouse prostate. The tumor growth was monitored noninvasively using the IVIS imaging system after the intraperitoneal (i.p) injection of D-luciferin. After minimal tumor growth, the mice were randomized into four groups ($n = 9$ or

(*Continued.*) **C,** Quantitative RT-PCR and Western blot analyses of PDE5 expression in Pten knockout mouse prostate tumor tissue-derived mRNA in comparison with age-matched wild-type mouse prostate tissue. **D,** Quantitative RT-PCR and Western blot analyses of PDE5 were performed in Pten knockout mouse prostate-derived cell lines. Western blot analyses of PDE5 expression in mouse cell lines were shown in the top panel. **E,** An ELISA was performed to determine the basal cGMP levels in prostate cancer cells. **F,** For the ELISA, 22Rv1 prostate cancer cells were plated in a 6-well format at a concentration of 5×10^4 cells/cm^2, allowed to grow, and then treated with increasing concentrations of sildenafil (Sild) for 30 minutes. The resulting cells were lysed and analyzed for cGMP levels. For the Western blot analysis, a duplicate set of experiments was performed to determine PDE5 expression levels. **G,** 22Rv1 prostate cancer cells were treated with various concentrations of docetaxel and combination with sildenafil, and cGMP levels were measured. As compared with untreated control (first column), cGMP levels are significantly higher in docetaxel (Doce) and docetaxel sildenafil combination treatment. **H,** 22Rv1 prostate cancer cells were treated with docetaxel and the relative NO levels were determined using DAF-FM diacetate. The relative NO levels (fluorescent benzotriazole derivative) in live cells were quantified by a fluorescent plate reader (left). A representative fluorescent image is shown in the right. **I,** qRT-PCR for *NOS2* mRNA levels in 22Rv1 prostate cancer cells treated with different concentrations of docetaxel for 72 hours. **J,** 22Rv1 prostate cancer cells were treated with docetaxel and 1400W (NOS2-specific inhibitor) alone or in the combination and analyzed for NO production by a fluorescent plate reader (left) and fluorescent microscope (right). **K,** 22Rv1 prostate cancer cells were treated with docetaxel and 1400W (NOS2 inhibitor) alone or in the combination and analyzed for cGMP levels by ELISA. Scale bar, 200 μm. cGMP, cyclic guanosine monophosphate; DAF-FM diacetate, 4-amino-5-methylamino-2′,7′-difluorescein diacetate; DEA, diethylamine NONOate (NO donor, positive control); Doce, docetaxel; GC, guanylate cyclase; NO, nitric oxide; NOS2, nitric oxide synthase 2. 0.5, 1, and 2 denote the concentration in nmol/L and μmol/L of docetaxel and sildenafil, respectively. Data are expressed as mean ± SEM.

Downloaded from http://aacrjournals.org/clincancerres/article-pdf/26/21/5720/2064320/5720.pdf by guest on 28 August 2022

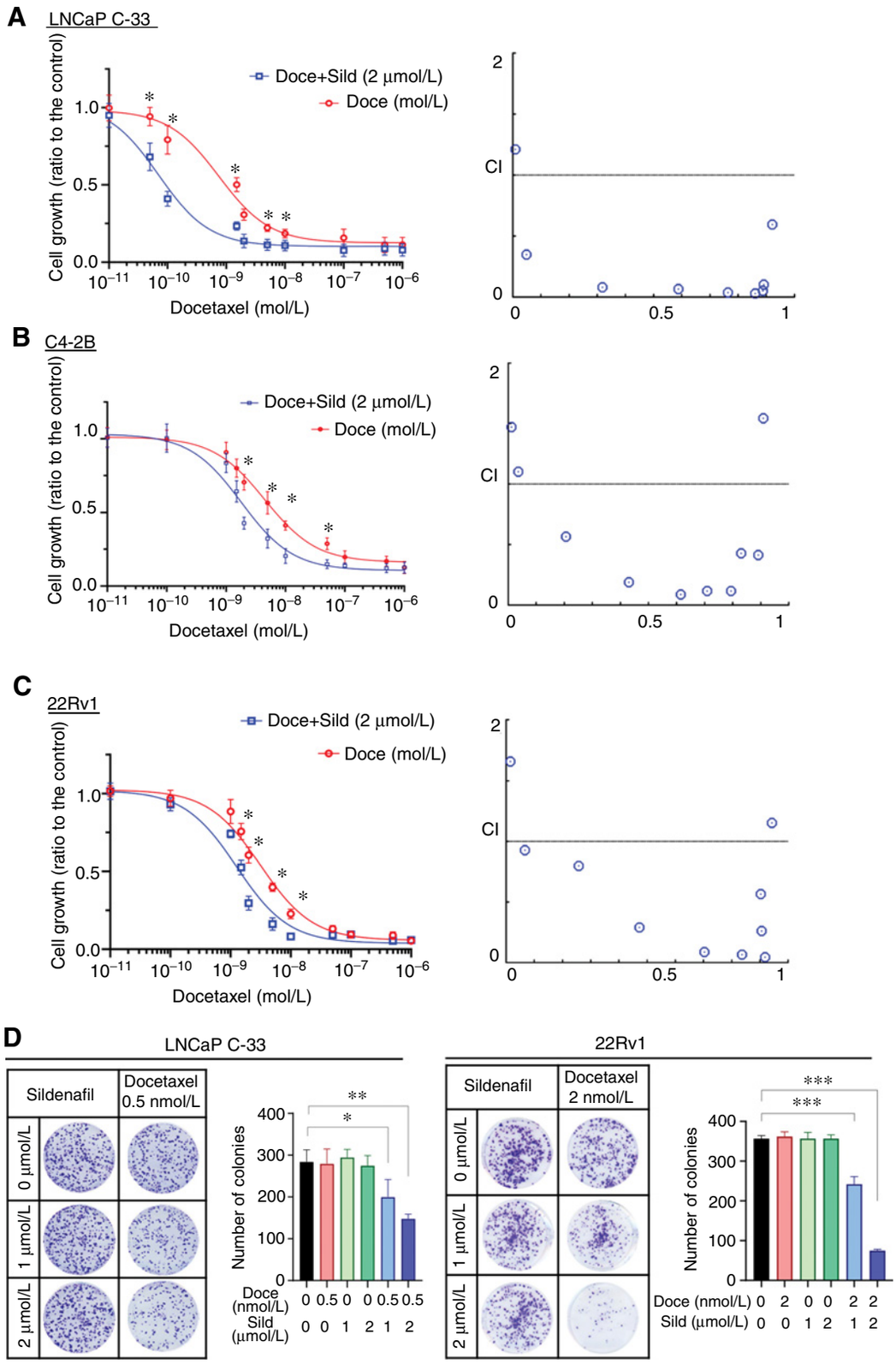

Figure 2.

Sildenafil (Sild) enhances docetaxel (Doce)-induced prostate cancer cell death. The antiproliferative effects of docetaxel and sildenafil alone or in combination, were assessed in LNCaP C-33 (**A**), C4-2B (**B**), and 22Rv1 (**C**) prostate cancer cells. Prostate cancer cells were treated with docetaxel and sildenafil as indicated for 72 hours, replacing the treatment every 24 hours. (*Continued on the following page.*)

Downloaded from http://aacrjournals.org/clincancerres/article-pdf/26/21/5720/2064320/5720.pdf by guest on 28 August 2022

10/group). The control group received vehicle (saline). The second group of mice received docetaxel intraperitoneally at a concentration of 3 mg/kg body weight once in 3 days. The third group of mice received 5 mg/kg body weight sildenafil every 24 hours (i.p). The fourth group received docetaxel and sildenafil in combination; sildenafil was administered 30 minutes prior to docetaxel. Tumor growth and the therapeutic impact on mice were monitored and recorded twice weekly. On the basis of tumor growth, mice were sacrificed after 21 days, and the tumors and other vital organs were excised for further analyses.

IHC analyses

To determine the impact of sildenafil and docetaxel therapeutic combination on tissue toxicity, highly vascularized tissues were stained for hematoxylin and eosin (H&E). For Ki67 and cleaved caspase-3 IHC staining, tissue sections were warmed overnight at 56°C, deparaffinized, and rehydrated. Antigen retrieval was performed by boiling the tissue sections with citrate buffer (pH 6.0). After endogenous peroxidase was blocked with 3% H_2O_2 for an hour, nonspecific binding was blocked with normal goat serum, and sections were incubated with appropriate primary antibodies overnight. The sections were washed and incubated with an secondary antibody for an hour. The reactivity was visualized with 3,3′-diaminobenzidine (DAB) (Vector Laboratories). Hematoxylin was used as nuclear counterstain.

Statistical analysis

Statistical analyses were performed by GraphPad Prism (Version 8.4). The mean value for each parameter in each group were calculated and the results are expressed as mean ± SEM. Student *t* test was used to determine significant differences between two groups. One-way ANOVA followed by Tukey comparison were used for multiple comparisons among groups. $P \leq 0.05$ was considered statistically significant.

Results

Prostate cancer cells express functional PDE5 and both NO and PDE5 are essential for aberrant cGMP accumulation

To determine the effect of docetaxel on cGMP production, we first measured PDE5 expression and basal levels of cGMP in prostate cancer cells and tissues. PDE5 expression was profiled both at RNA and protein levels. In human prostate cancer tissue, mean *PDE5* transcript levels were 50% higher than in normal/benign tissue (**Fig. 1A**). Significantly higher expression of *PDE5* in prostate cancer vs. normal was also observed in publically available datasets (Supplementary Fig. S1A and S1B) (27, 28). *PDE5* expression levels were highest in prostate cancer among various cancers (Supplementary Fig. S1C and S1D) (29). PDE5 expression levels varied between prostate cancer cell lines, and expression was observed in a majority of the prostate cancer cell lines tested (Supplementary Fig. S1E). Interestingly, many AR-positive prostate cancer cell lines expressed detectable *PDE5* RNA and protein except the VCaP cells (**Fig. 1B**). Supportively, in genetically engineered mouse (GEM) prostate (**Fig. 1C**) and GEM prostate tumor–derived cancer cell lines (**Fig. 1D**), PDE5 expression levels were higher when compared with normal prostate and $Pten^{wt}$ cells, respectively. Interestingly, the PDE5 levels were in increasing trend from normal to androgen-dependent and castrated prostate derived cell lines (**Fig. 1D**).

Similarly, cGMP levels were detectable in all three prostate cancer cell lines examined (**Fig. 1E**). Intracellular levels of cGMP depend on the balance between the rate of synthesis through guanylate cyclase (GC) and degradation controlled by PDEs (PDE5). Hence, we determined the independent effects of sildenafil and docetaxel on cGMP levels. The PDE5 inhibitor sildenafil alone (up to 100 μmol/L) did not have a significant effect on cGMP level or PDE5 protein expression (**Fig. 1F**). On the other hand, docetaxel alone induced cGMP levels by 10-fold in 22Rv1 prostate cancer cells. The addition of 2 μmol/L of sildenafil to docetaxel treatment further increased cGMP levels (**Fig. 1G**; $P < 0.05$) when compared with docetaxel alone.

cGMP is generally produced by NO/sGC-mediated signaling (Supplementary Fig. S2A). To assess the effect of docetaxel on NO production, we treated 22Rv1 prostate cancer cells with docetaxel and quantified NO (fluorescent benzotriazole derivative) in live cells by both fluorescent plate reader and fluorescent imaging system. Starting at 2 nmol/L, docetaxel induced NO generation, increasing the intensity with higher concentrations (**Fig. 1H**). Nitrite and nitrate accumulation were assessed as an alternative measure of NO released in the culture medium. As shown in Supplementary Fig. S2B, docetaxel induced NO release in 22Rv1 prostate cancer cells. Furthermore, we determined the levels of inducible nitric oxide synthesis (iNOS, also called NOS2), whose induction depends on external stimuli in 22Rv1 prostate cancer cells. As expected, docetaxel treatment significantly increased NOS2 expression levels even after 72 hours (**Fig. 1I**). To determine the effect of sildenafil on upstream NO levels, 22Rv1 cells were treated with docetaxel and sildenafil. Sildenafil did not have an additional effect on NO levels (Supplementary Fig. S2C). To determine whether docetaxel-induced NO production is through NOS2, we used NOS2-specific inhibitor 1400W (Medchem Express) in the presence and absence of docetaxel. Addition of 1400W abrogated docetaxel-induced NO generation (**Fig. 1J**). To further determine the impact of NOS2 blockage on cGMP accumulation, we performed a similar treatment and analyzed for cGMP levels. The addition of docetaxel significantly increased cGMP levels (**Fig. 1K**). Treatment with 1400W inhibited docetaxel-induced cGMP production in 22Rv1 prostate cancer cells. All these results indicate that at least in prostate cancer cells, cGMP synthesis depends on upstream NO-mediated signaling. Its accumulation is governed by the combined action of upstream NO/GC signaling and PDE5 inhibition.

(*Continued.*) The left side indicates the drug response curve plotted using Graph Pad Prism. The *y*-axis indicates the live-cell ratio, and the *x*-axis indicates the dosage of drugs in molar concentration. The sigmoidal curve shows the dose-response in prostate cancer cells. The bottom line indicates the cell growth response to docetaxel and sildenafil, and the top line indicates the response to docetaxel alone. The right side of each panel indicates the combinational index (CI) plot as determined by CompuSyn online software (Chou-Talalay method; ref. 25). The CI plot illustrates the synergistic effect of docetaxel and sildenafil when less than 2 μmol/L of sildenafil is combined with either 0.5 nmol/L (for LNCaP C-33) or 2 nmol/L (C4-2B and 22Rv1) of docetaxel in prostate cancer cells. A combination index <1 indicates synergism, = 1 indicates an additive effect, and >1 indicates an antagonistic effect. **D,** Effect of docetaxel and sildenafil combination on clonogenic growth of LNCaP C-33 and 22Rv1 prostate cancer cells. Left, clonogenic growth; right, the mean number of clones in each group. Data are represented as mean ± SEM. Doce, docetaxel; Sild, sildenafil and 0.5, 1, and 2 denotes the concentration in nmol/L and μmol/L of docetaxel and sildenafil, respectively.

Downloaded from http://aacrjournals.org/clincancerres/article-pdf/26/21/5720/2064320/5720.pdf by guest on 28 August 2022

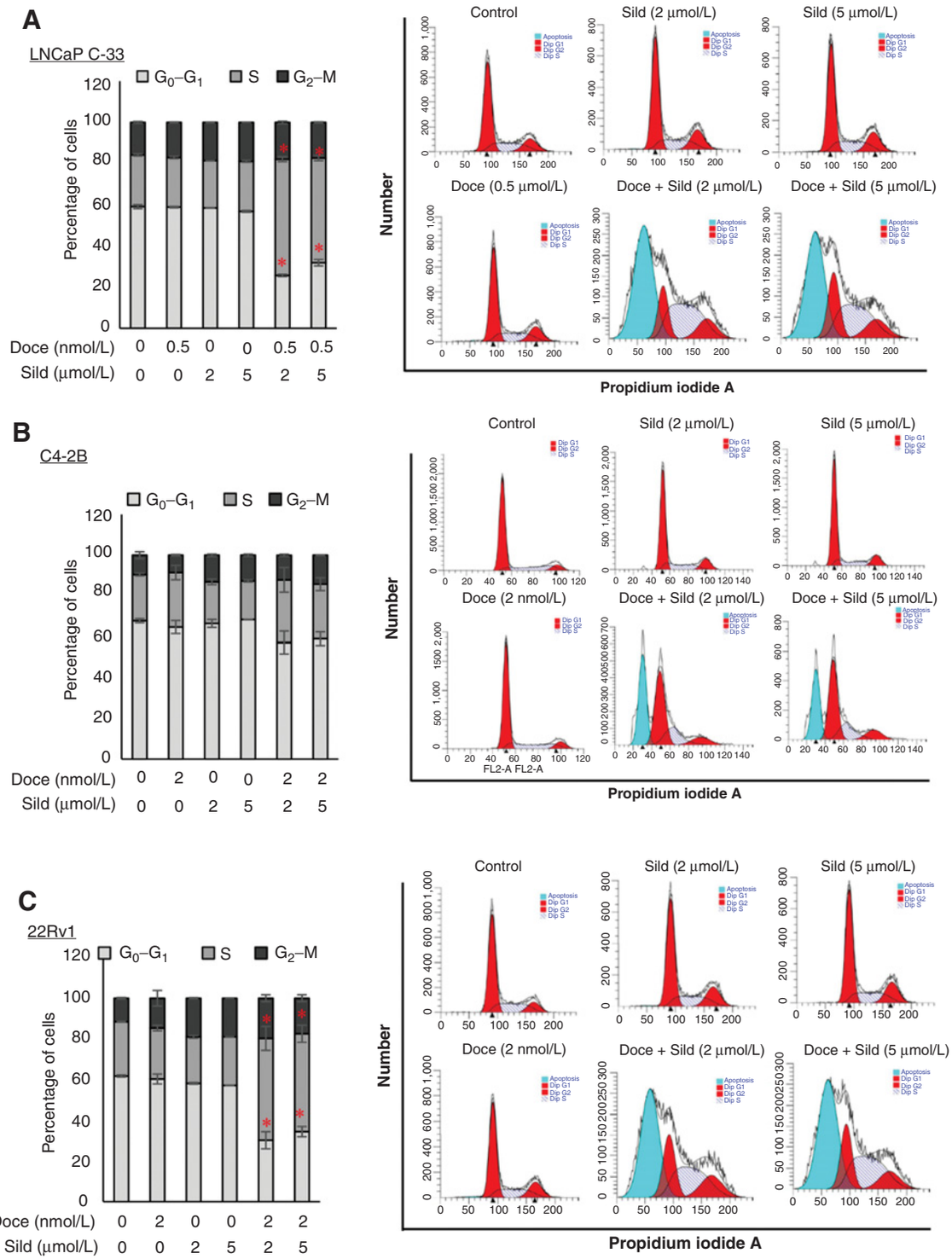

Figure 3.

Effect of docetaxel (Doce) and sildenafil (Sild) combination on the prostate cancer cell-cycle profile. LNCaP (**A**), C4-2B (**B**), and 22Rv1 (**C**) prostate cancer cells treated with indicated concentrations of either docetaxel or sildenafil alone or in combination for 72 hours. Cells were then trypsinized, fixed, and stained with propidium iodide (PI) for at least 30 minutes. PI-stained cells were analyzed by flow cytometry to determine the percentage of cells in each phase of the cell cycle (left). The bar diagram on the left shows the overall percentage of LNCaP C-33 (**A**), C4-2B (**B**), and 22Rv1 (**C**) prostate cancer cells in each phase of the cell cycle. Each histogram on the right side represents a group to depict the overall percentage of prostate cancer cells in particular phase of the cell cycle. Data represent the mean ± SEM from two independent experiments with triplicate samples.

Downloaded from http://aacrjournals.org/clincancerres/article-pdf/26/21/5720/2064320/5720.pdf by guest on 28 August 2022

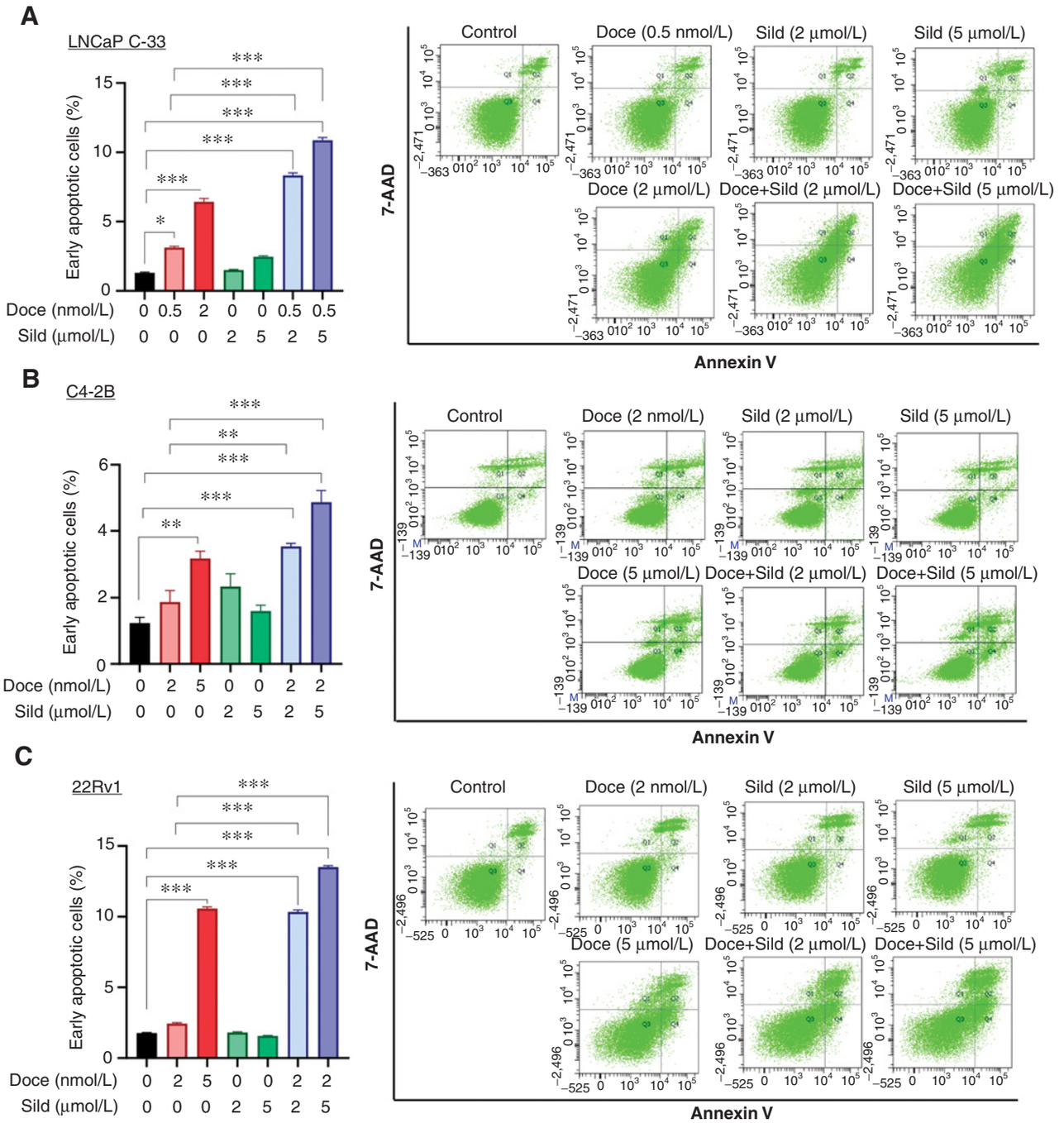

Figure 4.

Sildenafil (Sild) significantly enhances docetaxel (doce)–mediated cellular apoptosis in prostate cancer cells. LNCaP C-33, C4-2B, and 22Rv1 prostate cancer cells were treated with the indicated concentrations for 72 hours. The phosphatidylserine externalization in LNCaP C-33 (**A**), C4-2B (**B**), and 22Rv1 (**C**) prostate cancer cells was determined by Annexin V/7-AAD staining using FACS. The bar diagram represents the percentage of early apoptotic cells. Scatterplots depict each treatment group. The bar diagram on the left bottom shows the overall percentage of early apoptotic (Annexin V positive, 7-AAD negative) cells from two independent experiments with triplicate samples.

Sildenafil enhances docetaxel-induced cell death

Cell growth analysis showed that docetaxel inhibited cell growth in a dose-dependent manner in all three (LNCaP C-33, C4-2B, and 22Rv1) prostate cancer cell lines (**Fig. 2A–C**, left). Prostate cancer cell lines showed slight variations in dose responses to docetaxel (0.5 to 2 nmol/L). Interestingly, treatment with sildenafil alone did not result in growth inhibition of all three (LNCaP C-33, C4-2B, and 22Rv1) prostate cancer cell lines tested until 100 μmol/L (Supplementary

Downloaded from http://aacrjournals.org/clincancerres/article-pdf/26/21/5720/2064320/5720.pdf by guest on 28 August 2022

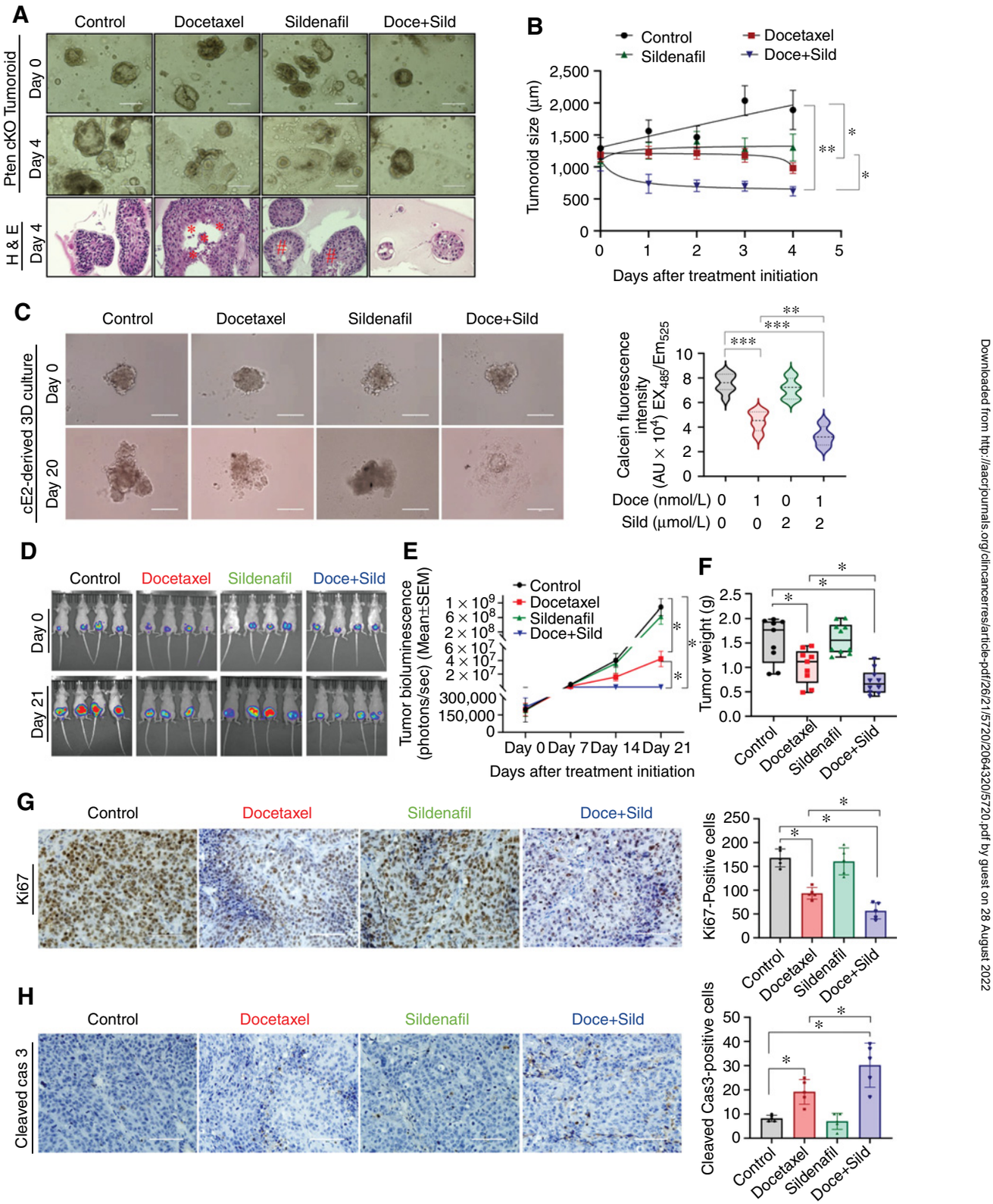

Figure 5.

Sildenafil (Sild) enhances the therapeutic benefit of docetaxel in an *in vivo* orthotopic prostate cancer model and mouse prostate cancer cell lines. **A,** Pten conditional knockout (cKO) mouse prostate-derived tumoroids were cultured and randomly assigned for either docetaxel (Doce) or sildenafil (sild) alone or the combination treatment. (*Continued on the following page.*)

Downloaded from http://aacrjournals.org/clincancerres/article-pdf/26/21/5720/2064320/5720.pdf by guest on 28 August 2022

Fig. S3). In contrast, the addition of 2 μmol/L sildenafil to docetaxel substantially enhanced cell growth inhibition (**Fig. 2A–C**). The combination index (CI) plot confirms the synergistic effect of the combination (**Fig. 2A–C**, right). Furthermore, the addition of the IC_{25} dose of docetaxel intensified the effect of sildenafil combination on cell growth inhibition, confirming the synergistic effect (Supplementary Fig. S3).

The efficacy of docetaxel and sildenafil on prostate cancer cells was determined by anchorage-dependent colony formation assay. When compared with the untreated control, treatment with the IC_{25} dose of docetaxel for 10 days did not have significant effect on established colonies from both LNCaP C-33 and 22Rv1 prostate cancer cells (**Fig. 2D**). In contrast, the combination of sildenafil and docetaxel (IC_{25} dose) treatment for 10 days significantly reduced colony numbers. Again, at the therapeutic level, sildenafil alone did not have an appreciable effect on both cell types (**Fig. 2D**).

Combination of sildenafil and docetaxel blocks cells at G_0–G_1

On the basis of the dose–response results for docetaxel and sildenafil, next, we performed cell-cycle analyses on LNCaP C-33, C4-2B, and 22Rv1 prostate cancer cells. Cells were treated for 72 hours with docetaxel (IC_{25} concentration) and sildenafil (2 or 5 μmol/L) alone or the combination. In untreated conditions, the majority of the prostate cancer cells were in the G_1 phase, followed by G_2–M and S phases. Neither docetaxel (IC_{25}) nor sildenafil alone (2 and 5 μmol/L) had a significant effect on cell-cycle profiles in LNCaP C-33, C4-2B, and 22Rv1 prostate cancer cells (**Fig. 3A–C**). However, the combination of docetaxel and sildenafil treatment arrested a large percentage of cells in the sub-G_0 phase with an observable change in S, G_2–M, and a significant decrease in G_1 phase (**Fig. 3A–C**, histogram). In both cell lines, the higher dose of sildenafil (5 μmol/L vs. 2 μmol/L) in combination with docetaxel did not further increase the frequency in sub-G_0. Interestingly, in the combination groups alone, a significant amount of cells were at the sub G_0–G_1 phase, which indicates the apoptotic effect of the treatment combination. These results suggest that the combination acts synergistically to induce cell-cycle arrest, which was not observed with either of the drugs alone.

Addition of sildenafil enhances docetaxel-induced early apoptotic cells

On the basis of the strong synergistic effect of combined docetaxel and sildenafil on cell proliferation and cell-cycle profiles, we assessed apoptosis using the annexin V assay. Flow cytometry analysis showed that the docetaxel and sildenafil combination significantly promoted apoptosis (annexin V^+) in prostate cancer cells (**Fig. 4A–C**). Quantitative analysis showed that docetaxel alone dose-dependently increased the total number of apoptotic cells, but not sildenafil treatment. The results show that the apoptotic effects of the treatments are similar among LNCaP C-33, C4-2B, and 22Rv1 prostate cancer cells (**Fig. 4**).

Combination of sildenafil and docetaxel treatment shows therapeutic benefit in syngeneic cell lines, Pten cKO–derived tumoroids, and *in vivo* xenograft model

In both syngeneic mouse cE1 (Supplementary Fig. S4A) and cE2 prostate cancer cell lines (Supplementary Fig. S4B), sildenafil enhanced the effect of docetaxel on cell growth inhibition. Furthermore, the decrease in live cells was supported by increased caspase-3 cleavage and PARP cleavage detected in cE2 cells (Supplementary Fig. S4C). In both cE1 and cE2 cell lines, sildenafil alone did not significantly affect cell growth. To study the impact of therapeutic intervention in 3D setting, we used our recently developed Pten cKO–derived tumoroids (23). Compared with no-drug control tumoroids, both sildenafil and docetaxel prevented further growth in the tumoroid throughout the treatment period (**Fig. 5A** and **B**). However, sildenafil treatment did not achieve statistical significance. However, the combination treatment greatly reduced tumoroid size and growth and was statistically significant when compared with both untreated control and docetaxel alone–treated tumoroid groups (**Fig. 5A** and **B**). Histologic examination of H&E-stained tumoroid sections revealed that the control tumoroid maintains the integrity of the tumoroid structure and the epithelial cell morphology. The sildenafil-treated groups showed condensed structure with occasional apoptosis, vacuole formation. The docetaxel alone–treated tumoroids showed structural disintegration and marked necrotic cells. The combination treatment completely reduced tumoroid size and growth, with condensed structure, loss of integrity, structural blebbing, and apoptosis (**Fig. 5A** and **B**). As represented in **Fig. 5C**, in epithelial cell–derived three-dimensional setting, sildenafil alone did not show a significant difference in colony growth. We observed that docetaxel alone or the combination of docetaxel and sildenafil showed a profound effect on colony size (**Fig. 5C**, right). Furthermore, the docetaxel and sildenafil combination showed significantly reduced colony size as indicated by reduced fluorescence and colony disintegration (**Fig. 5C**).

To further highlight the relevance of the combination treatment, we orthotopically implanted luciferase-labeled C4-2B prostate cancer cells into immunodeficient male nude mice. LNCaP C-33 is poorly tumorigenic *in vivo*. 22Rv1 prostate cancer cells have AR splice variant (v7), whose presence remains controversial with respect to docetaxel response in xenograft studies (30). Hence, we chose LNCaP C-33 androgen-independent variant, C4-2B prostate cancer cells to perform the xenograft study. Individual tumor growth and therapy responses over the period were recorded every week using IVIS imaging until the animals were sacrificed. As shown in **Fig. 5D** and **E**, the bioluminescence signal intensity was observably lower in both the docetaxel and docetaxel plus sildenafil groups when compared with control; the mice treated with sildenafil alone did not show any difference in bioluminescence compared with control mice. However, the mice treated with docetaxel sildenafil combination showed significantly reduced

(*Continued.*) The top image represents the randomization image, and the respective middle image shows the same organoid growth after the treatment. Scale bar, 1,000 μm. Representative tumoroid culture were preserved and processed for H&E (bottom image) to determine structural integrity. **B,** Pten cKO–derived tumoroids were monitored every 24 hours, and the size were measured throughout the treatment period. **C,** Pten cKO prostate tumor–derived cE2 cells were used to generate 3D culture and treated with either docetaxel or sildenafil alone or in the combination for 20 days (left). Scale bar, 400 μm. The three-dimensional cultures were briefly exposed to calcein-AM to determine the relative live cell concentrations. **D,** Luciferase-tagged C4-2B prostate cancer cells were implanted orthotopically in the prostate of immunocompromised nude mice ($n = 9/10$ per group), and the tumor growth was monitored invasively over time, as indicated. The top panel of images was captured at the time of randomization, and the bottom panel IVIS image was taken the day before sacrifice. **E,** C4-2B prostate cancer cells implanted mice were monitored invasively during the experimental period, and the total luminescence intensity was calculated as total photon flux/second. **F,** Tumors were excised, weighed, and plotted as a box plot. Each dot represents an individual tumor weight. Tumors were fixed with 10% buffered formalin, sectioned, and stained for Ki67 (**G**), a proliferative marker, and cleaved caspase-3 (**H**). Bar diagram depicts the Ki67 and cleaved caspase-3–positive cells were quantified from 10 representative images, Scale bar, 200 μm.

Downloaded from http://aacrjournals.org/clincancerres/article-pdf/26/21/5720/2064320/5720.pdf by guest on 28 August 2022

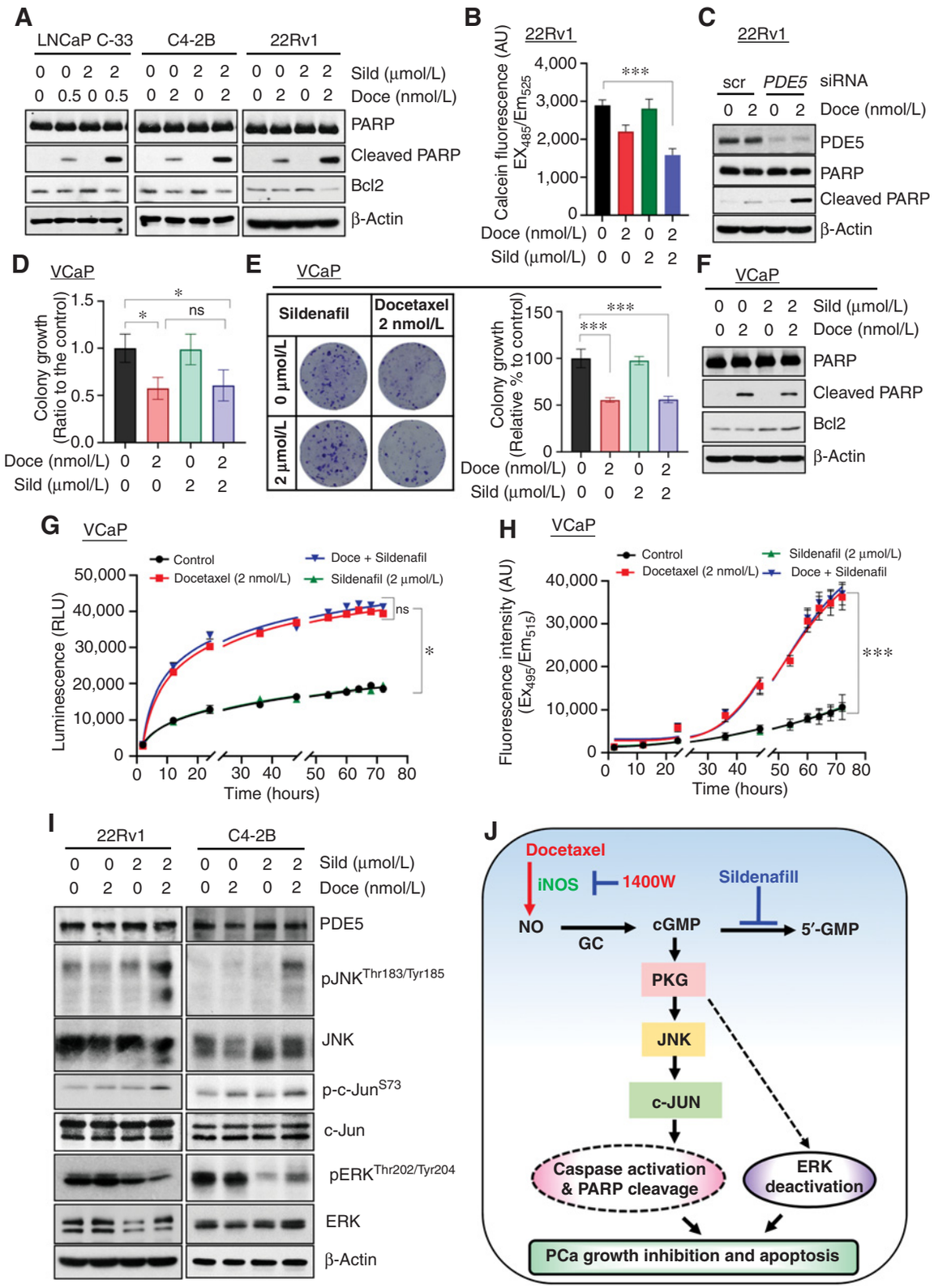

Figure 6.

PDE5 blocking by sildenafil (Sild) enhances docetaxel (Doce) efficacy on prostate cancer (PCa) cells. A separate set of LNCaP C-33, C4-2B, and 22Rv1 (**A**) prostate cancer cells were treated with either docetaxel or sildenafil alone or in combination for 72 hours and processed for PARP cleavage determination by immunoblot analyses. (*Continued on the following page.*)

Downloaded from http://aacrjournals.org/clincancerres/article-pdf/26/21/5720/2064320/5720.pdf by guest on 28 August 2022

bioluminescence compared with docetaxel alone–treated mice (**Fig. 5E**). Subsequently, the mice were sacrificed, and the prostate tumor was resected and weighed. As shown in **Fig. 5F**, when compared with the control group, the mean tumor weight was significantly lower in docetaxel-treated mice, but not in the sildenafil-treated group. Similar to the *in vitro* observations, the addition of sildenafil to docetaxel resulted in significantly ($P < 0.05$) lower tumor weight than all other groups (**Fig. 5F**). Again, sildenafil alone did not have a significant effect on tumor growth compared with control mice.

To determine the apoptotic phenotype at the cellular level, we stained prostate xenograft tissues with the proliferative marker Ki67, and with cleaved caspase-3, the effector caspase in the apoptotic pathway. The percentage of Ki67-positive nuclei was significantly lower in tumors derived from docetaxel-treated mice. In the combination group, Ki67 staining was considerably lower when compared with groups treated with individual drugs (**Fig. 5G**). On the other hand, cleaved caspase-3 staining was increased in the docetaxel-treated tumor. Furthermore, the frequency of cleaved caspase-3–positive cells was higher in the combination group compared with docetaxel alone (**Fig. 5H**). On par with *in vitro* observations, sildenafil alone did not have a significant effect on Ki67 and cleaved caspase-3 immunostaining (**Fig. 5G** and **H**).

Presence of PDE5 is essential for docetaxel-induced PARP cleavage and cell death

To further characterize the cellular effects of the drug treatments, we assessed cleaved PARP levels *in vitro* by immunoblotting. Combined treatment with docetaxel and sildenafil increased PARP cleavage, and the effect was higher than with docetaxel alone (**Fig. 6A**) in LNCaP C-33, C4-2B, and 22Rv1 prostate cancer cells. Importantly, docetaxel at the treated concentration showed less effect on PARP cleavage than the combination treatment. On par with cell-cycle and annexin V assay results (**Figs. 3** and **4**), sildenafil alone did not induce PARP cleavage at a detectable level in any of the prostate cancer cell lines examined (**Fig. 6A**). To identify the molecular mechanism behind sildenafil and docetaxel synergy, we assessed the MPTP opening, which controls the release of proapoptotic molecules (31). As expected, docetaxel treatment caused prolonged MPTP opening, as indicated by reduced calcein-AM fluorescence. The combination of docetaxel and sildenafil further decreased calcein-AM fluorescence (**Fig. 6B**). The collective results suggest that increased mitochondrial pore opening may contribute to the higher PARP cleavage, which could result in higher apoptosis with the combination treatment.

To test the hypothesis that PDE5 inhibition would specifically recapitulate the added efficacy of sildenafil, we used siRNA-mediated PDE5 knockdown (KD) in 22Rv1 prostate cancer cells. PDE5 siRNA transfection resulted in significant PDE5 downregulation (**Fig. 6C**). We next treated the PDE5 KD cells with docetaxel. As seen in **Fig. 6C**, PDE5 KD enhanced the effect of docetaxel on PARP cleavage. As expected, sildenafil did not add any additional efficacy in PDE5-negative VCaP cells (**Fig. 6D**). The selective effect of docetaxel alone was captured well in VCaP colony growth (**Fig. 6E**) and docetaxel-mediated PARP cleavage and Bcl2 expression levels (**Fig. 6F**). To determine the impact of docetaxel and sildenafil combination on VCaP cell viability, we performed the Real-Time-Glo Annexin V apoptosis and necrosis assay. As shown in **Fig. 6G**, docetaxel treatment induced apoptosis within 24 hours and the amount of apoptosis plateaued at a later time point in VCaP cells. The addition of sildenafil alone or the combination did not induce or enhanced apoptosis (**Fig. 6G**). Similarly, in VCaP prostate cancer cells, docetaxel induced necrosis after 48 hours and it persisted until the analyses (**Fig. 6H**).

PDE5 inhibition reduces ERK phosphorylation and enhances docetaxel-induced JNK activation

Under physiologic conditions, cGMP-dependent protein kinase activation (PKG) results in a myriad of downstream signaling modulations such as JNK, ERK, β-catenin, etc (32). Sildenafil treatment for 72 hours reduced ERK phosphorylation in both C4-2B and 22Rv1 prostate cancer cells. The decrease in ERK phosphorylation was also observed with combined sildenafil and docetaxel treatment, but not with docetaxel treatment alone (**Fig. 6I**). On the other hand, docetaxel alone induced JNK-mediated c-Jun phosphorylation, but not with sildenafil alone. Whereas, the combination of docetaxel and sildenafil further increased the JNK and its downstream c-Jun phosphorylation (**Fig. 6I**). Furthermore, we have observed that docetaxel can induce NO-mediated cGMP, and its levels were further increased by the addition of sildenafil (**Fig. 1**). Supportively, we observed increased PARP cleavage, and reduced Bcl2 expression in sildenafil and docetaxel combination groups but not with sildenafil treatment alone. Although the potential mechanisms by which NO/cGMP mediate apoptosis need to be explored further, our results along with evidence in literature suggest that upregulated cGMP levels may activate PKG, which can execute its antitumorigenic function through its downstream proteins such as JNK and ERK, etc. These reduced levels of phospho-ERK may be accompanied by the induction of apoptosis, contributing to the effects of the combination on reduced cell growth (**Fig. 6J**).

Discussion

For the first time, this study shows the therapeutic benefit of docetaxel and sildenafil combination in human and mouse prostate cancer cells. Multiple pieces of clinical evidence support the significance of using sildenafil and docetaxel combination in prostate cancer: (i) despite the modest therapeutic improvement with docetaxel

(*Continued.*) **B,** Mitochondrial permeability transition pore opening was determined by calcein/$CoCl_2$ fluorescence in 22Rv1 prostate cancer cells. The calcein fluorescence product was read at 488/525 nm using a fluorescent plate reader. **C,** 22Rv1 prostate cancer cells were transfected with PDE5-specific siRNAs or scrambled siRNAs. 22Rv1 prostate cancer cells were then treated with or without docetaxel. After 72 hours, the cells were lysed and analyzed for PDE5 and cleaved PARP expression by immunoblot. **D,** The growth pattern of PDE5-negative VCaP cells in response to docetaxel and sildenafil combination. **E,** Effect of docetaxel and sildenafil combination on clonogenic growth of VCaP prostate cancer cells. Left, clonogenic growth; right, the relative colony growth determined in each group. **F,** Docetaxel- and sildenafil-treated VCaP prostate cancer cells were analyzed for PARP cleavage and Bcl2 expression levels. **G,** PS exposure (luminescence) patterns of VCaP prostate cancer cells treated with or without docetaxel and sildenafil alone or the combination. The luminescence intensity was measured periodically with the replenishment of drugs, reagents, and media every 24 hours. **H,** The loss of membrane integrity (a measure of apoptosis) of VCaP prostate cancer cells was measured after the cells received docetaxel and sildenafil alone or the combination treatment. **I,** Immunoblot analyses of 22Rv1 prostate cancer cells show decreased ERK activation and increased JNK/c-Jun phosphorylation in response to combination treatment. **J,** Schematic representation shows docetaxel and sildenafil cooperatively induce apoptosis mediated by the second messenger cGMP, and inhibit cell growth. Data are represented as mean ± SEM. 0.5, 1, and 2 denote the concentration in nmol/L and μmol/L of docetaxel and sildenafil, respectively.

Downloaded from http://aacrjournals.org/clincancerres/article-pdf/26/21/5720/2064320/5720.pdf by guest on 28 August 2022

chemotherapy, most patients become nonresponsive and develop resistance, which limits prostate cancer patient survival (2, 4, 6); (ii) adverse events following docetaxel administration are common, especially in real-world experience (33–36), and typically are managed with dose reductions or treatment holidays; and (iii) PDE5 expression is higher in prostate cancer (**Fig. 1A**), which is further supported by our Oncomine analysis showing that PDE5 expression is highest in prostate among various tumors (Supplementary Fig. S1).

In response to cellular stress such as docetaxel, various proteins such as BCL-2 family members, Bax, caspases, and PARP can modulate the rate of proliferation and cell death. The observed Annexin V^+ and PARP cleavage patterns in the present study suggest that sildenafil might enhance docetaxel-induced apoptosis, partly explaining the reduced cell growth in response to combined sildenafil and docetaxel (**Fig. 2**). The calcein-AM fluorescence assay results further suggest that the observed apoptosis may be preceded by decreased mitochondrial membrane potential and longer MPTP opening, which may subsequently release apoptosis-inducing factor and cytochrome *c* to initiate apoptosis through PARP and caspase-3 activation (31). We observed a significant change in growth and apoptotic patterns in the docetaxel-treated group, which was enhanced with the addition of sildenafil in contrast to the groups treated with sildenafil alone. These results suggest that sildenafil could synergistically enhance the antitumor activity of docetaxel in prostate cancer cells. The *in vivo* tumor growth and the IHC changes in the xenograft tissues supported this notion (**Fig. 5**). In Pten cKO–derived tumoroid cultures, sildenafil alone able to maintain the size and growth of the tumoroids. However, sildenafil alone did not inhibit the growth of cE2 mouse syngeneic cell line (Pten cKO derived) formed 3D cultures (**Fig. 5**). The discrepancy between the results may be due to the presence of stroma and other cell types. As prostate smooth muscle cells are known to express higher levels of PDE5, which may dictate the sildenafil treatment outcome, possibly preventing hypoxia-induced myofibroblast activation (8).

Combinational strategies with docetaxel in mCRPC have not resulted in a clinical benefit to date (7, 8). One reason could be that most of the combination therapies previously tested considered multiple agents without an overlapping target, with the reasoning that the drugs would attack from multiple directions. Our results suggest that a subtherapeutic dose of docetaxel and a physiologically achievable sildenafil concentration could synergize by increasing cGMP to inhibit cell growth and induce apoptosis (**Figs. 1** and **2**). Notably, PDE5 overexpression is observed in various cancers, including breast carcinomas (10) and bladder squamous carcinoma (11), where sildenafil is shown to have antitumorigenic efficacy. Likewise, sildenafil has been shown to enhance the antitumor activity of kinase inhibitors in multiple cancer cell lines (37). The efficacy of sildenafil depends on PDE5 expression, and PDE5 has been detected in the heart, lung, intestine, bladder, muscle, and brain, in addition to the prostate (38). In our study, mice treated with sildenafil alone or in combination with docetaxel appear normal, as no change in their overall body weight (Supplementary Fig. S5), and no microscopical abnormalities in the vascularized tissues such as liver, kidney, lung, and colon (Supplementary Fig. S5B), indicating a lack of recognizable toxicity. Hence, having shown that PDE5 is functional in prostate cancer cells and druggable with clinically available drugs like sildenafil, the approach used in this study could be feasible to manage advanced prostate cancer in the clinic.

The results from various tumor models have demonstrated that sildenafil can inhibit tumors either directly by inducing cGMP-mediated PKG activation or indirectly through DNA damage, which leads to tumor growth inhibition and apoptosis induction (32, 39–42). It has also been shown that sildenafil can potentiate doxorubicin-induced, ROS-mediated apoptosis in PC-3, and DU145 prostate cancer cells by upregulating caspase activity and downregulating Bcl family members (15). Furthermore, it has been shown that the effect of sildenafil and doxorubicin may occur through the death receptor CD95 (16). Although all these studies demonstrate the therapeutic benefits through enhancing the chemotherapeutic efficacy through apoptosis, this study reveals upstream signaling for the combined synergistic action of docetaxel and sildenafil. On the other hand, a recent study has shown that sildenafil did not add the therapeutic efficacy in lung cancer cell lines (43). This differential effect might be due to cell types, availability of internal binding partners, nitric oxide receptors (sGC), and other internal survival factors. Furthermore, docetaxel alone is known to have therapeutic potential; however, as observed in our study (**Fig. 2**), at higher concentrations of docetaxel, sildenafil is not shown to induce significant efficacy over docetaxel alone. The clear understanding for the opposing effects needs further study.

At the cellular level, docetaxel can induce NO (**Fig. 1**), which in turn may increase cGMP through GC (32), which is further supported by the abolishment of docetaxel-induced cancer cell death by blocking NOS2 with 1400W (**Fig. 1K**). NO is a gaseous signaling molecule, whose synthesis and consumption depend on NOS and GC, depending on tissue and disease context (44). Constitutively active neuronal NOS1 and endothelial NOS3 can induce NO production at nanomolar levels (44). In contrast, iNOS (NOS2) is induced by external stimuli to produce NO at micromolar concentrations, mostly in macrophages and cancer cells (45). In this study, the induction of NOS2 by docetaxel may account for the increased NO levels (**Fig. 1**). Consistent with these points, cGMP levels were further increased by the addition of sildenafil to docetaxel treatment, but not by sildenafil alone, which suggests that upstream NO signaling is essential for the synthesis of cGMP (46, 47).

The stabilized cGMP can exert its action through downstream cGMP-dependent PKG, ion channels, and cGMP-regulated PDEs (47, 48). It has been suggested that NO can activate JNK directly (47, 49) or indirectly through PKG (50), which can lead to caspase activation and apoptosis. Our results suggest that the drug combination may prefer a cGMP-dependent mechanism over direct action for inducing cell growth arrest and apoptosis. This is supported by the proposal that direct activation of JNK requires a higher concentration of NO and is likely to proceed at a slower pace (kinetics) than for cGC-mediated cGMP production (51). The increased cGMP levels by the combination treatment could potentially explain the decreased ERK activation, which is supported by the recent observation that sildenafil could enhance C-type natriuretic peptide (CNP)-mediated antiproliferative effects by inhibiting the Raf/MEK/ERK pathway in rhabdomyosarcoma cells (52). Overall, the combined action of docetaxel and sildenafil on prostate cancer cell proliferation and apoptosis could be multifactorial. On the one hand, the NO-mediated cGMP increase could induce apoptosis. On the other hand, cGMP levels could be further stabilized through PDE5 inhibition with sildenafil. Downstream, the increased cGMP levels may also lead to downstream alteration of ERK and JNK phosphorylation levels. The combined actions of these events may both reduce cell proliferation and induce apoptosis (**Fig. 6J**).

We used 2 μmol/L of sildenafil for the study, rather than 100 μmol/L, the IC_{50}. This dose is justified by the observation that 100 mg oral administration in healthy individuals translated to a serum sildenafil concentration of 440 ng/mL (53). In addition, our results show that 2 μmol/L of sildenafil is sufficient to increase cGMP levels significantly. The increased cGMP levels were paralleled by increased apoptosis and

Downloaded from http://aacrjournals.org/clincancerres/article-pdf/26/21/5720/2064320/5720.pdf by guest on 28 August 2022

cell growth inhibition when tested in combination with docetaxel. Hence, the 2 μmol/L sildenafil dose in cell culture media could be reasonable based on the maximal prescribed dose of 100 mg, and physiochemical and pharmacokinetic properties of the drug such as solubility, stability, and half-life.

Overall, our results demonstrate that the addition of sildenafil enhanced docetaxel-mediated cell death compared with docetaxel alone. The results suggest that the persistent supply of NO by docetaxel may be sufficient to induce cGMP, which can be stabilized through PDE5 inhibition and lead to enhanced therapeutic efficacy. Besides, PDE5 inhibition leads to reduced levels of ERK activation, which has favorable implications for cell growth inhibition. On the basis of our results, docetaxel and sildenafil (both are in clinic for prostate cancer and erectile dysfunction, respectively) could act synergistically through a common mechanism that could improve the therapeutic efficacy of docetaxel in patients with prostate cancer. Using this strategy, it may also be possible to reduce the docetaxel dose to minimize its toxicity without compromising therapeutic benefits and this approach may delay the development of chemoresistance in patients with advanced prostate cancer.

Disclosure of Potential Conflicts of Interest

No potential conflicts of interest were disclosed.

Authors' Contributions

S. Muniyan: Conceptualization, data curation, formal analysis, investigation, methodology, writing-original draft, project administration, writing-review and editing. **S. Rachagani:** Formal analysis, investigation, methodology, writing-review and editing. **S. Parte:** Formal analysis, validation, methodology, writing-review and editing. **S. Halder:** Formal analysis, investigation, methodology, writing-review and editing. **P. Seshacharyulu:** Data curation, formal analysis, investigation, methodology, writing-review and editing. **P. Kshirsagar:** Formal analysis, validation, methodology, writing-review and editing. **J.A. Siddiqui:** Formal analysis, validation, methodology, writing-review and editing. **R. Vengoji:** Formal analysis, methodology, writing-review and editing. **S. Rauth:** Formal analysis, methodology, writing-review and editing. **R. Islam:** Formal analysis, investigation, methodology, writing-review and editing. **K. Mallya:** Formal analysis, investigation, methodology, writing-review and editing. **K. Datta:** Data curation, formal analysis, investigation, methodology, writing-review and editing. **L. Xi:** Data curation, formal analysis, investigation, methodology, writing-review and editing. **A. Das:** Data curation, formal analysis, investigation, methodology, writing-review and editing. **B.A. Teply:** Data curation, formal analysis, investigation, methodology, writing-review and editing. **R.C. Kukreja:** Conceptualization, data curation, formal analysis, funding acquisition, methodology, writing-review and editing. **S.K. Batra:** Conceptualization, resources, data curation, formal analysis, supervision, funding acquisition, methodology, writing-original draft, project administration, writing-review and editing.

Acknowledgments

The authors thank Dr. Jessica Mercer for her editorial contributions. The authors also acknowledge the University of Nebraska Medical Center (UNMC) Flow Cytometry Research Facility and Tissue Sciences Facility (TSF) for their resources and services. This work and the authors are, in part, supported by the NIH grant U01 CA185148 (to S.K. Batra); R01 CA221813, DK120866, HL118808 (to R.C. Kukreja) and R01 HL134366 (to R.C. Kukreja and A. Das), and Department of Defense Award W81XWH-18-1-0308 (PC170891; to S.K. Batra and R.C. Kukreja).

The costs of publication of this article were defrayed in part by the payment of page charges. This article must therefore be hereby marked *advertisement* in accordance with 18 U.S.C. Section 1734 solely to indicate this fact.

Received April 24, 2020; revised July 22, 2020; accepted August 17, 2020; published first August 26, 2020.

References

1. Tannock IF, de Wit R, Berry WR, Horti J, Pluzanska A, Chi KN, et al. Docetaxel plus prednisone or mitoxantrone plus prednisone for advanced prostate cancer. N Engl J Med 2004;351:1502–12.
2. Petrylak DP, Tangen CM, Hussain MH, Lara PN Jr, Jones JA, Taplin ME, et al. Docetaxel and estramustine compared with mitoxantrone and prednisone for advanced refractory prostate cancer. N Engl J Med 2004;351:1513–20.
3. Herbst RS, Khuri FR. Mode of action of docetaxel - a basis for combination with novel anticancer agents. Cancer Treat Rev 2003;29:407–15.
4. Al-Batran SE, Van Cutsem E, Oh SC, Bodoky G, Shimada Y, Hironaka S, et al. Quality-of-life and performance status results from the phase III RAINBOW study of ramucirumab plus paclitaxel versus placebo plus paclitaxel in patients with previously treated gastric or gastroesophageal junction adenocarcinoma. Ann Oncol 2016;27:673–9.
5. de Morree ES, Vogelzang NJ, Petrylak DP, Budnik N, Wiechno PJ, Sternberg CN, et al. Association of survival benefit with docetaxel in prostate cancer and total number of cycles administered: a post Hoc analysis of the mainsail study. JAMA Oncol 2017;3:68–75.
6. de Morrée E, van Soest R, Aghai A, de Ridder C, de Bruijn P, Ghobadi Moghaddam-Helmantel I, et al. Understanding taxanes in prostate cancer; importance of intratumoral drug accumulation. Prostate 2016;76:927–36.
7. Corn PG, Agarwal N, Araujo JC, Sonpavde G. Taxane-based combination therapies for metastatic prostate cancer. Eur Urol Focus 2019;5:369–80.
8. Teply BA, Hauke RJ. Chemotherapy options in castration-resistant prostate cancer. Indian J Urol 2016;32:262–70.
9. Watson PA, Arora VK, Sawyers CL. Emerging mechanisms of resistance to androgen receptor inhibitors in prostate cancer. Nat Rev Cancer 2015;15:701–11.
10. Catalano S, Campana A, Giordano C, Gyorffy B, Tarallo R, Rinaldi A, et al. Expression and function of phosphodiesterase type 5 in human breast cancer cell lines and tissues: implications for targeted therapy. Clin Cancer Res 2016;22:2271–82.
11. Piazza GA, Thompson WJ, Pamukcu R, Alila HW, Whitehead CM, Liu L, et al. Exisulind, a novel proapoptotic drug, inhibits rat urinary bladder tumorigenesis. Cancer Res 2001;61:3961–8.
12. Whitehead CM, Earle KA, Fetter J, Xu S, Hartman T, Chan DC, et al. Exisulind-induced apoptosis in a non-small cell lung cancer orthotopic lung tumor model augments docetaxel treatment and contributes to increased survival. Mol Cancer Ther 2003;2:479–88.
13. Sarfati M, Mateo V, Baudet S, Rubio M, Fernandez C, Davi F, et al. Sildenafil and vardenafil, types 5 and 6 phosphodiesterase inhibitors, induce caspase-dependent apoptosis of B-chronic lymphocytic leukemia cells. Blood 2003;101:265–9.
14. Zhu B, Vemavarapu L, Thompson WJ, Strada SJ. Suppression of cyclic GMP-specific phosphodiesterase 5 promotes apoptosis and inhibits growth in HT29 cells. J Cell Biochem 2005;94:336–50.
15. Das A, Durrant D, Mitchell C, Mayton E, Hoke NN, Salloum FN, et al. Sildenafil increases chemotherapeutic efficacy of doxorubicin in prostate cancer and ameliorates cardiac dysfunction. Proc Natl Acad Sci U S A 2010;107:18202–7.
16. Das A, Durrant D, Mitchell C, Dent P, Batra SK, Kukreja RC. Sildenafil (Viagra) sensitizes prostate cancer cells to doxorubicin-mediated apoptosis through CD95. Oncotarget 2016;7:4399–413.
17. Booth L, Roberts JL, Cruickshanks N, Conley A, Durrant DE, Das A, et al. Phosphodiesterase 5 inhibitors enhance chemotherapy killing in gastrointestinal/genitourinary cancer cells. Mol Pharmacol 2014;85:408–19.
18. Black KL, Yin D, Ong JM, Hu J, Konda BM, Wang X, et al. PDE5 inhibitors enhance tumor permeability and efficacy of chemotherapy in a rat brain tumor model. Brain Res 2008;1230:290–302.
19. Chavez AH, Scott Coffield K, Hasan Rajab M, Jo C. Incidence rate of prostate cancer in men treated for erectile dysfunction with phosphodiesterase type 5 inhibitors: retrospective analysis. Asian J Androl 2013;15:246–8.
20. Mimeault M, Rachagani S, Muniyan S, Seshacharyulu P, Johansson SL, Datta K, et al. Inhibition of hedgehog signaling improves the anti-carcinogenic effects of docetaxel in prostate cancer. Oncotarget 2015;6:3887–903.
21. Muniyan S, Chen SJ, Lin FF, Wang Z, Mehta PP, Batra SK, et al. ErbB-2 signaling plays a critical role in regulating androgen-sensitive and castration-resistant androgen receptor-positive prostate cancer cells. Cell Signal 2015;27:2261–71.

Downloaded from http://aacrjournals.org/clincancerres/article-pdf/26/21/5720/2064320/5720.pdf by guest on 28 August 2022

22. Muniyan S, Chou YW, Ingersoll MA, Devine A, Morris M, Odero-Marah VA, et al. Antiproliferative activity of novel imidazopyridine derivatives on castration-resistant human prostate cancer cells. Cancer Lett 2014;353:59–67.
23. Seshacharyulu P, Rachagani S, Muniyan S, Siddiqui JA, Cruz E, Sharma S, et al. FDPS cooperates with PTEN loss to promote prostate cancer progression through modulation of small GTPases/AKT axis. Oncogene 2019;38:5265–80.
24. Liao CP, Liang M, Cohen MB, Flesken-Nikitin A, Jeong JH, Nikitin AY, et al. Mouse prostate cancer cell lines established from primary and postcastration recurrent tumors. Horm Cancer 2010;1:44–54.
25. Chou TC. Drug combination studies and their synergy quantification using the Chou-Talalay method. Cancer Res 2010;70:440–6.
26. Vengoji R, Macha MA, Nimmakayala RK, Rachagani S, Siddiqui JA, Mallya K, et al. Afatinib and Temozolomide combination inhibits tumorigenesis by targeting EGFRvIII-cMet signaling in glioblastoma cells. J Exp Clin Cancer Res 2019;38:266.
27. Tomlins SA, Mehra R, Rhodes DR, Cao X, Wang L, Dhanasekaran SM, et al. Integrative molecular concept modeling of prostate cancer progression. Nat Genet 2007;39:41–51.
28. Wallace TA, Prueitt RL, Yi M, Howe TM, Gillespie JW, Yfantis HG, et al. Tumor immunobiological differences in prostate cancer between African-American and European-American men. Cancer Res 2008;68:927–36.
29. Ramaswamy S, Tamayo P, Rifkin R, Mukherjee S, Yeang CH, Angelo M, et al. Multiclass cancer diagnosis using tumor gene expression signatures. Proc Natl Acad Sci U S A 2001;98:15149–54.
30. Zhang G, Liu X, Li J, Ledet E, Alvarez X, Qi Y, et al. Androgen receptor splice variants circumvent AR blockade by microtubule-targeting agents. Oncotarget 2015;6:23358–71.
31. Tait SW, Green DR. Mitochondria and cell death: outer membrane permeabilization and beyond. Nat Rev Mol Cell Biol 2010;11:621–32.
32. Das A, Durrant D, Salloum FN, Xi L, Kukreja RC. PDE5 inhibitors as therapeutics for heart disease, diabetes and cancer. Pharmacol Ther 2015;147:12–21.
33. Nader R, El Amm J, Aragon-Ching JB. Role of chemotherapy in prostate cancer. Asian J Androl 2018;20:221–9.
34. Chin SN, Wang L, Moore M, Sridhar SS. A review of the patterns of docetaxel use for hormone-resistant prostate cancer at the Princess Margaret Hospital. Curr Oncol 2010;17:24–9.
35. Markman M. Managing taxane toxicities. Support Care Cancer 2003;11:144–7.
36. Kushnir I, Koczka K, Ong M, Canil C, Bosse D, Sabri E, et al. The timing of docetaxel initiation in metastatic castrate-sensitive prostate cancer and the rate of chemotherapy-induced toxicity. Med Oncol 2019;36:18.
37. Booth L, Albers T, Roberts JL, Tavallai M, Poklepovic A, Lebedyeva IO, et al. Multi-kinase inhibitors interact with sildenafil and ERBB1/2/4 inhibitors to kill tumor cells *in vitro* and *in vivo*. Oncotarget 2016;7:40398–417.
38. Lin CS. Tissue expression, distribution, and regulation of PDE5. Int J Impot Res 2004;16:S8–S10.
39. Li N, Xi Y, Tinsley HN, Gurpinar E, Gary BD, Zhu B, et al. Sulindac selectively inhibits colon tumor cell growth by activating the cGMP/PKG pathway to suppress Wnt/beta-catenin signaling. Mol Cancer Ther 2013;12:1848–59.
40. Mei XL, Yang Y, Zhang YJ, Li Y, Zhao JM, Qiu JG, et al. Sildenafil inhibits the growth of human colorectal cancer in vitro and in vivo. Am J Cancer Res 2015;5:3311–24.
41. Islam BN, Sharman SK, Hou Y, Bridges AE, Singh N, Kim S, et al. Sildenafil suppresses inflammation-driven colorectal cancer in mice. Cancer Prev Res 2017;10:377–88.
42. Chang JF, Hsu JL, Sheng YH, Leu WJ, Yu CC, Chan SH, et al. Phosphodiesterase type 5 (PDE5) inhibitors sensitize topoisomerase II inhibitors in killing prostate cancer through PDE5-independent impairment of HR and NHEJ DNA repair systems. Front Oncol 2018;8:681.
43. Domvri K, Zarogoulidis K, Zogas N, Zarogoulidis P, Petanidis S, Porpodis K, et al. Potential synergistic effect of phosphodiesterase inhibitors with chemotherapy in lung cancer. J Cancer 2017;8:3648–56.
44. Mungrue IN, Bredt DS, Stewart DJ, Husain M. From molecules to mammals: what's NOS got to do with it? Acta Physiol Scand 2003;179:123–35.
45. Lind M, Hayes A, Caprnda M, Petrovic D, Rodrigo L, Kruzliak P, et al. Inducible nitric oxide synthase: good or bad? Biomed Pharmacother 2017;93:370–5.
46. Russwurm M, Russwurm C, Koesling D, Mergia E. NO/cGMP: the past, the present, and the future. Methods Mol Biol 2013;1020:1–16.
47. Murad F. Shattuck Lecture. Nitric oxide and cyclic GMP in cell signaling and drug development. N Engl J Med 2006;355:2003–11.
48. Lucas KA, Pitari GM, Kazerounian S, Ruiz-Stewart I, Park J, Schulz S, et al. Guanylyl cyclases and signaling by cyclic GMP. Pharmacol Rev 2000;52:375–414.
49. Wagner EF, Nebreda AR. Signal integration by JNK and p38 MAPK pathways in cancer development. Nat Rev Cancer 2009;9:537–49.
50. Soh JW, Mao Y, Kim MG, Pamukcu R, Li H, Piazza GA, et al. Cyclic GMP mediates apoptosis induced by sulindac derivatives via activation of c-Jun NH2-terminal kinase 1. Clin Cancer Res 2000;6:4136–41.
51. Keshet R, Erez A. Arginine and the metabolic regulation of nitric oxide synthesis in cancer. Dis Model Mech 2018;11:dmm033332.
52. Zenitani M, Nojiri T, Uehara S, Miura K, Hosoda H, Kimura T, et al. C-type natriuretic peptide in combination with sildenafil attenuates proliferation of rhabdomyosarcoma cells. Cancer Med 2016;5:795–805.
53. Nichols DJ, Muirhead GJ, Harness JA. Pharmacokinetics of sildenafil after single oral doses in healthy male subjects: absolute bioavailability, food effects and dose proportionality. Br J Clin Pharmacol 2002;53:5S–12S.

Downloaded from http://aacrjournals.org/clincancerres/article-pdf/26/21/5720/2064320/5720.pdf by guest on 28 August 2022